Jurnal
Teknologi

Full Paper

DESIGN AND ANALYSIS OF A SINUSOIDAL PWM RECTIFIER CIRCUIT UNDER DIFFERENT OPERATING CONDITIONS

Rakan Khalil ANTAR

Northern Technical University, Technical Engineering College, Mosul, Iraq

Article history
Received
8 November 2023
Received in revised form
22 August 2024
Accepted
21 September 2024
Published Online
28 April 2025

Corresponding author
rakan.antar@ntu.edu.iq

Graphical abstract

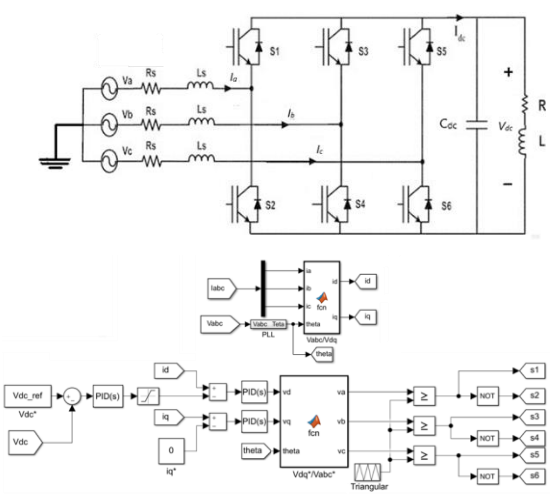

Abstract

In this study, a sinusoidal PWM rectifier is designed and modeled to enhance the performance of the system under different operating conditions. The system is tested under balanced AC sources and various loads. It is also tested under unbalanced and distorted three-phase AC sources. The key performance goal of the suggested system is to minimize the total harmonic distortion (THD) of the supply AC current while maintaining a unity power factor. The proposed controller is designed to drive the IGBTs and generate the required output DC voltage with minimal THD and a power factor of unity. The designed system and controller were simulated, and the obtained results demonstrate good power quality. The system showed decreased THD and a unity power factor across various loads, as well as under stable and unstable conditions in both steady-state and transient conditions. The maximum THD value is 3.8992% at 600Vdc, while the minimum THD value is 0.3867% at 1200Vdc. These values are achieved with an almost unity power factor under all conditions. These results demonstrate the effectiveness of the proposed system in dynamic operations.

Keywords: Sinusoidal PWM rectifier, PI controller, total harmonic distortion, power factor, balanced and unbalanced conditions

1.0 INTRODUCTION

A PWM (Pulse Width Modulation) rectifier is a power electronic circuit that converts alternating current (AC) voltage to direct current (DC) voltage. It offers several advantages, including improved efficiency, reduced harmonic distortion, and better power quality. This is done with the help of diodes or thyristors. These converters are reliable, easy to configure, and inexpensive to manufacture. Many disadvantages, such as low power factor (PF), high total harmonic distortion (THD), one-way power flow, a source of harmonics, and low power quality problems, are noted [1]. To solve these problems, a sinusoidal PWM rectifier (SPWMR) based on IGBT or MOSFET switches is utilized. Silicon carbide switches with high voltage/current and frequency ratings can be used [2]. SPWMRs are widely used in various applications, including motor drives, power supplies, renewable energy systems, and two-way energy flow [3]. They offer several advantages over conventional rectifier circuits, including high efficiency, low harmonic distortion, smaller size, and the ability to control the output voltage and power factor [4]. The PWM technique controls the switching of the IGBTs in the rectifier to closely resemble a pure sine wave in the AC input current waveform. By varying the width of the pulses, it is possible to control the average DC voltage output, enabling smooth and precise regulation of the output voltage. The boost-type PWM rectifier (BPWMR) has been increasingly utilized in recent years due to its ability to provide low AC current THD and a power factor close to unity at various loads, as well as the option for reverse flow power. The design and modelling of a SPWMR are important for several reasons, particularly in the field of power electronics and electrical engineering. It is used in applications where maintaining a high-quality AC power source is crucial. These rectifiers help reduce harmonics and distortion in the input current waveform, which can otherwise cause issues such as interference with other equipment, voltage fluctuations, and overheating of power distribution systems. Accurate modelling of the SPWMR enables precise control of the rectification process, including the fine-tuning of the modulation index and other parameters. This control is crucial in various applications, such as motor drives and renewable energy systems, for maintaining stability and efficiency.

Hartani *et al.*, (2010) proposed a control method using space vector pulse width modulation technique and utilizing two PI controllers to regulate the AC currents and the DC link voltage for a three-phase voltage source PWM rectifier [5]; Garasiya *et al.*, (2012) built a simulation and prototype PWM boost rectifier circuit model and the system produce a desirable boost in DC output voltage, maintenance of unity power factor at the input side, and THD less than 5% [6]; Koshti *et al.*, (2014) employed voltage-oriented control approach which utilizes two PI controllers for the SVPWM-based PWM rectifier to regulate the input AC current and the output DC voltage of the system [7]; Hassan *et al.*, (2015) suggested a control strategy to improve the performance of a PWM boost rectifier under different operating conditions of three-phase supply voltages (balanced, unbalanced, and distorted waves) [8]; while Qiang *et al.*, (2017) proposed a mathematical analysis of the three-phase voltage sourced PWM rectifier based on the rotating coordinate system, which relies on the space vector modulation algorithm [9]; Soe *et al.*, (2019) built a single-phase PWM rectifier with R and RL loads and the output voltage fluctuation is reduced by using the PI controller [10]; Hashemzade *et al.*, (2020) used a predictive control in a three-phase PWM rectifier to achieve simultaneous control of the active and reactive power of the converter [11]; in addition to that Song *et al.*, (2020) proposed a technique to reduce grid current distortions and simplify control systems [12]; while Yuksek *et al.*, developed a space vector PWM control system based on the d-q synchronous rotating axis set of the three-level rectifier [13]; Bie *et al.*, (2021) analyzed the construction and control approach of the PWM rectifier [14]; in the same year ISEN used hysteresis current control (HCC), sinusoidal pulse width modulation (SPWM), and voltage-oriented control (VOC) techniques in the rectifier circuit [15]; Li *et at*., (2022) constructed a three-phase PWM rectifier to enhance the dynamic response by implementing feed-forward decoupling and double closed-loop control [16]; in 2022, Wang *et at.* used a basic and improved model-free predictive current control with the PWM rectifier [17]; and in 2023, Zhou *et al.* established a PWM rectifier with d-q coordinate transformation and double closed-loop control systems [18].

As a continuation of the previous study, in order to obtain a complete understanding of power quality improvement in PWM rectifier systems, this study utilized a SPWM technique based on dq-theory and PI-controllers. The system is tested under various operating conditions, including both balanced and unbalanced networks. The novelty of the proposed SPWMR is that it effectively generates an output DC voltage with a high response and low input AC current harmonics. It also maintains a unity power factor during both balanced and unbalanced AC systems, regardless of the load and output. The main objective of this study is to improve the system's performance under various operating conditions.

2.0 METHODOLOGY

Modelling a SPWMR can be quite complex due to the nonlinear behaviour of semiconductor devices and the interaction between the PWM control and the electrical components. The modelling of a SPWMR requires creating a mathematical representation or a simulation of the circuit's behaviour. To successfully model a SPWMR, one must have a thorough understanding of the circuit topology. This includes establishing differential equations that represent the relationships between the input and output variables of the circuit, as well as incorporating an LC filter if necessary [19]. Additionally, it is important to implement a PWM switching control model based on the SPWM technique, describe PI controllers to regulate the output voltage or current, and simulate the system using MATLAB/Simulink in order to analyse the behaviour of the SPWMR model. The simulation model of the three-phase voltage source SPWMR structure is presented in Figure 1. A control strategy is implemented to regulate the DC bus voltage and achieve a unity power factor with high performance. This control strategy is implemented using PI controllers. SPWM is a modulation technique used in power electronics to generate a PWM signal with high-quality output waveforms and low harmonic distortion. A sinusoidal reference signal representing the desired output waveform has a fixed frequency and amplitude, which is compared with the high-frequency triangular carrier signal at each instant. Figure 2 represents the suggested control circuit. The conversion from abc to dq is used to convert three-phase currents (I_a, I_b, and I_c) into two-phase currents (I_d, I_q), which are often more convenient for analysis and control [20].

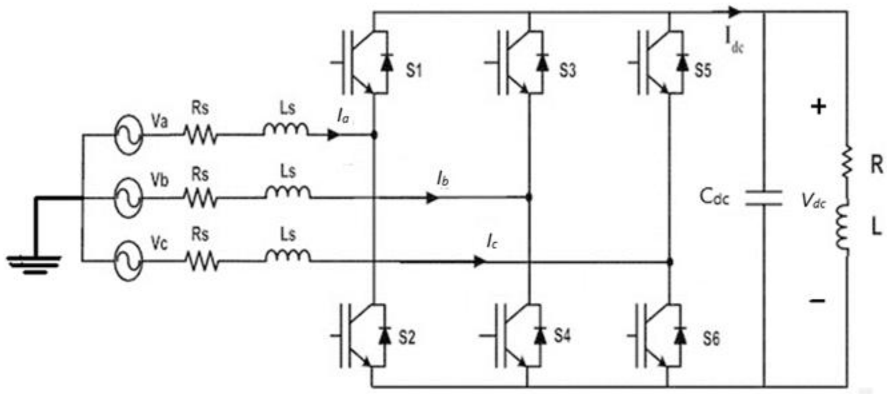

Figure 1 The block diagram of the proposed three-phase SPWMR

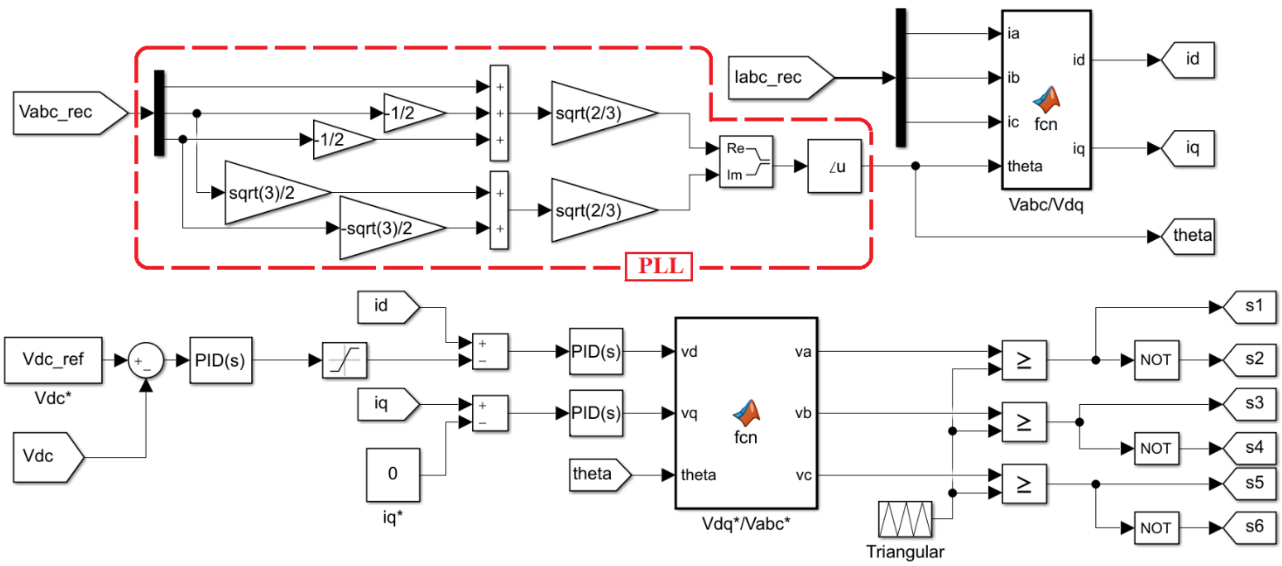

Figure 2 The SPWM controller circuit block diagram

$$Iq = \frac{-2}{3}\left(I_a \sin(\theta) + I_b \sin\left(\theta - \frac{2\pi}{3}\right) + I_c \sin\left(\theta + \frac{2\pi}{3}\right)\right) \quad (1)$$

$$Id = \frac{2}{3}\left(I_a \cos(\theta) + I_b \cos\left(\theta - \frac{2\pi}{3}\right) + I_c \cos\left(\theta + \frac{2\pi}{3}\right)\right) \quad (2)$$

A phase-locked loop (PLL) is a control system used in various applications to generate or synchronize a signal with a reference signal. The phase angle (θ) is calculated based on the principle of the PLL, which functions as a phase detector [21]. The control circuit utilizes an instantaneous PLL to quickly and accurately detect the angle of the AC power supply. The phase angle (θ) is detected as illustrated in Figure 2. The input of the first PI controller is the difference between the desired output DC voltage reference (V_{dc_ref}) and the measured output DC voltage (V_{dc}), which generates the reference d-axis current ($i_{d\text{-}ref}$). The input of the second PI controller is the difference between the reference d-axis current ($i_{d\text{-}ref}$) and the actual d-axis current (i_d). The output of this controller is then used as the input for the voltage PI controller, which generates the reference d-axis voltage ($v_{d\text{-}ref}$). The other third PI controller is used to generate the reference voltage (v_q) by subtracting the actual q-axis current (i_q) from the reference value, as shown in Figure 2. The Ki and Kp values of these three PI controllers are determined using trial and error method as illustrated in Table 1. After that, to return from dq to abc, the inverse transformation is used to generate the desired reference voltages ($v_{abc\text{-}ref}$). These reference voltages are compared with the triangular signal, and the resulting signals are the IGBT pulse signals. The significance of the proposed controller is to drive the IGBTs in order to produce the required DC voltage with unity power factor and minimize distortions in the AC supply currents.

$$v_{a-ref} = v_{d-ref} * \cos(\theta) - v_{q-ref} * \sin(\theta) \quad (3)$$

$$v_{b-ref} = v_{d-ref} * \cos\left(\theta - \frac{2\pi}{3}\right) - v_{q-ref} * \sin\left(\theta - \frac{2\pi}{3}\right) \quad (4)$$

$$v_{c-ref} = v_{d-ref} * \cos\left(\theta + \frac{2\pi}{3}\right) - v_{q-ref} * \sin\left(\theta + \frac{2\pi}{3}\right) \quad (5)$$

3.0 RESULTS AND DISCUSSION

To validate and fine-tune the proposed model and controller, various tests are conducted under different operating conditions. These tests include transient and steady-state analysis to observe the behaviour of the SPWMR in balanced system and load variations, as well as in unbalanced and distorted scenarios. Fine-tuning the model parameters is important to closely match the observed behaviour as accurately as possible. The suggested circuit, shown in Figure 1 and Figure 2, is simulated using MATLAB. The simulation is conducted with the selected parameters described in Table 1, assuming balanced voltage sources. The test is conducted with 12 types of loads, as explained in Table 2. The three-phase operation system has been tested to demonstrate the effectiveness and performance of the suggested circuit and controller. Figure 3 shows the flowchart of the suggested circuit and controller working steps.

Table 1 Parameters of the suggested three-phase SPWMR

Parameters	Values
Three-phase AC voltage sources V_a, V_b, V_c	220 V
Frequency	50 Hz
Source inductance (Ls) and resistance (Rs)	2mH and 50mΩ
DC side capacitor C_{dc}	1500 µF
Switching carrier frequency	5kHz
First PI controller	$K_{P1} = 5$, $K_{I1} = 50$
Second PI controller	$K_{P2} = 2000$, $K_{I2} = 100$
Third PI controller	$K_{P3} = 2000$, $K_{I3} = 100$

Table 2 Types of used loads

Loads	Loads	Loads
1. 50 Ω	5. 100Ω	9. 200Ω
2. 50Ω+50mH	6. 100Ω+50mH	10. 200Ω+50mH
3. 50Ω+100mH	7. 100Ω+100mH	11. 200Ω+100mH
4. 50Ω+200mH	8. 100Ω+200mH	12. 200Ω+200mH

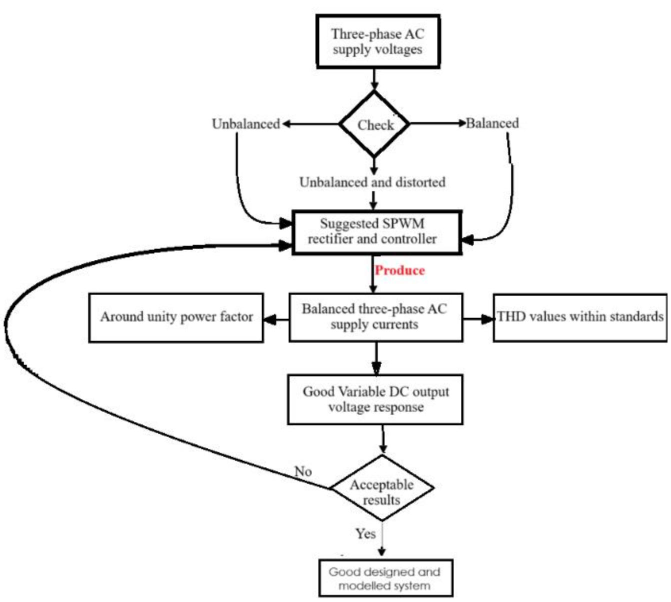

Figure 3 Flow chart of the suggested circuit and controller

3.1 Balanced AC voltage Sources

In this case, the system is tested using balanced voltage sources (220V, 50Hz) under various loads, as shown in Table 1 and Table 2. Figure 4(a) shows the AC supply currents at a Vdc of 800V and three different loads (50Ω+100mH, 100Ω+100mH, and 200Ω+100mH). The Fast Fourier Transform (FFT) analysis of these currents is explained in Figure 4(b). The THD values of the AC supply current at 800Vdc with three loads are 0.53%, 1.127%, and 2.1%, respectively. It can be seen from these results that all harmonic components are almost zero, which explains the effectiveness of the suggested circuit and controller. The input power factor is 0.998. The DC voltage response at 800V and different load values exhibits a nearly identical response, as depicted in Figure 5. Figure 6 shows the THD values at various voltage levels and loads. This figure explains that the THD values are within IEEE standards [22], which demonstrates the robustness of the designed circuit and controller. That means the system provided better THD at higher voltage levels, but had higher THD at lower DC voltage levels. The maximum THD value is 3.8992% at a voltage of 600Vdc and a load of 200Ω. The minimum THD value is 0.3867% at a voltage of 1200Vdc and a load of 50Ω+50mH. This happens due to less switching stress at higher voltages and lower loads. To evaluate the performance of the system, which is dependent on the output responses, various output voltage levels at different loads, as depicted in Figure 7. This figure illustrates that the system exhibits fast responses, indicating high system performance. The transient and steady-state responses of the three-phase AC currents at different DC output voltage levels, including a zoom section, are shown in Figure 8. To assess the system responses during load changes, Figure 9 illustrates the DC output voltage and current, as well as the phase AC supply voltage and current at 800Vdc. This waveform explains that the system has fast responses and high power quality. The apparent power (S), active power (P), reactive power (Q), and distortion power (D) are calculated to verify the performance of the system. These powers are calculated using equations defined by [23].

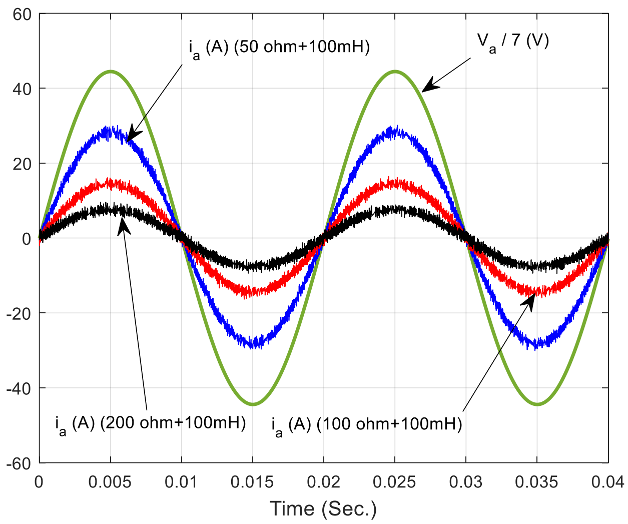

(a)

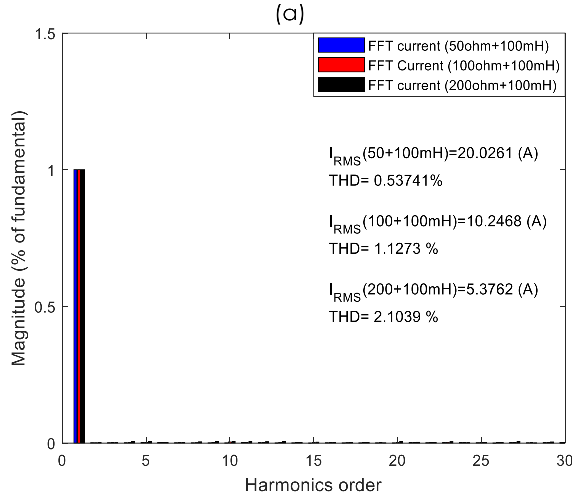

(b)

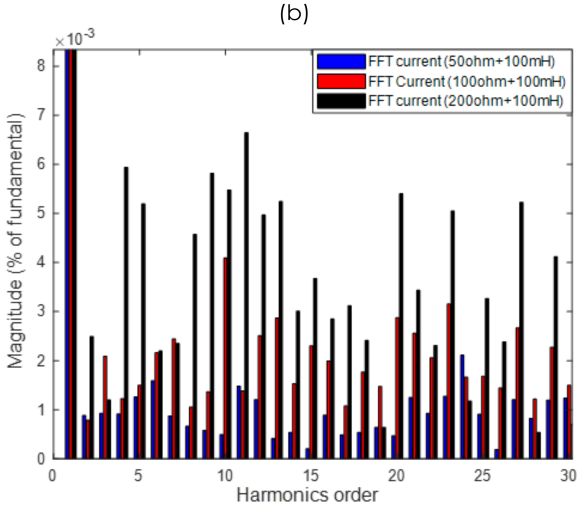

(c)

Figure 4 (a) AC supply voltage and currents waveforms at different loads (b) FFT currents analyzer, and (c) it's zoom section of the harmonic's component

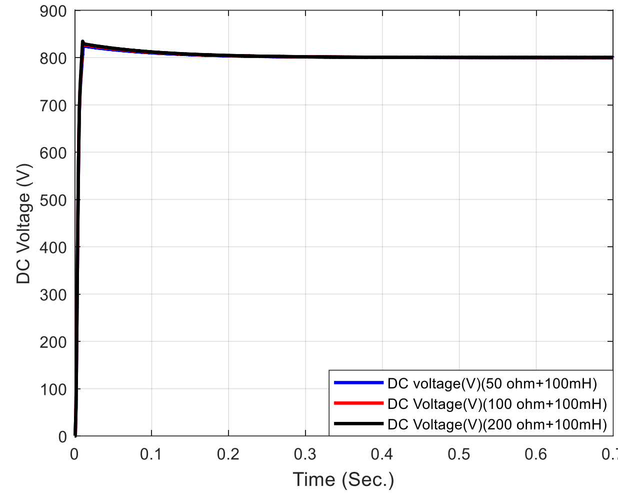

Figure 5 The output DC voltage response at 800V and different load values

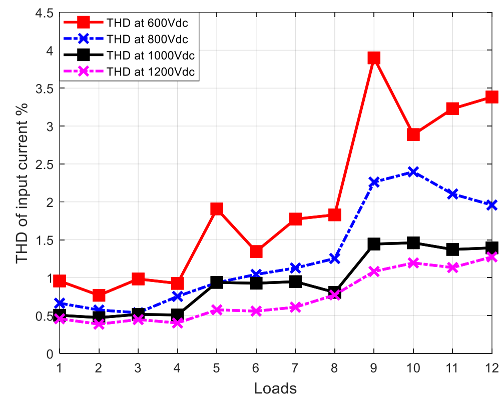

Figure 6 The THD waveform at different output DC voltages and loads

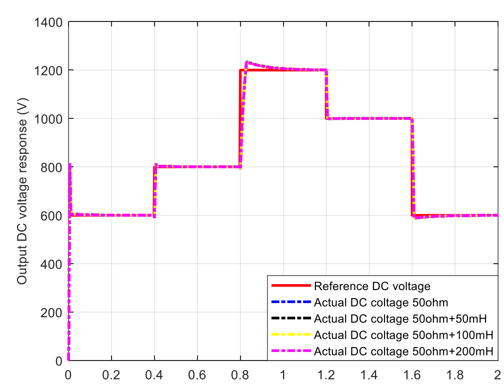

(a)

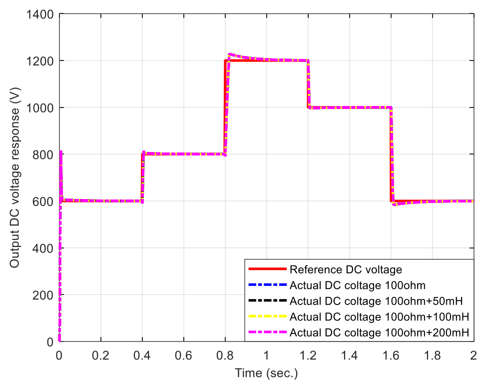

(b)

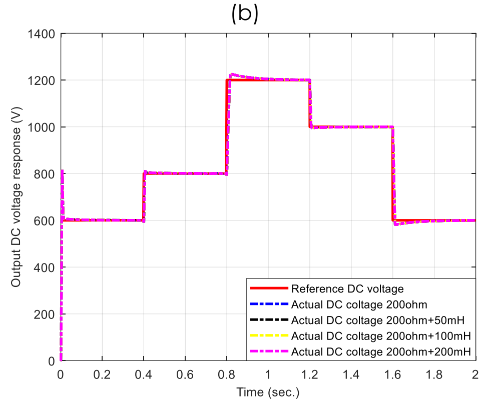

(c)

Figure 7 Different DC voltage responses at (a) 50Ω and different inductive values, (b) 100Ω and different inductive values, (c) 200Ω and different inductive values

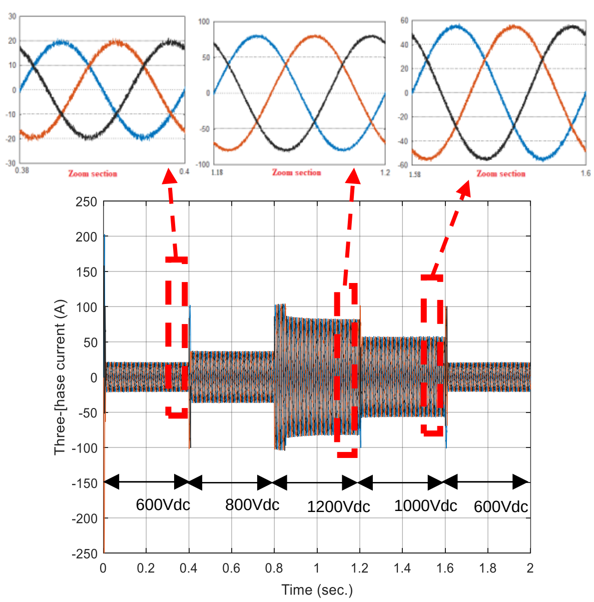

Figure 8 The three-phase AC supply currents at different output DC voltages with zoom section

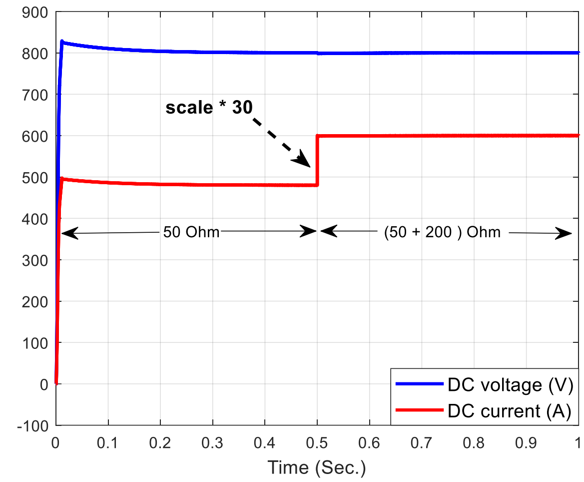

(a)

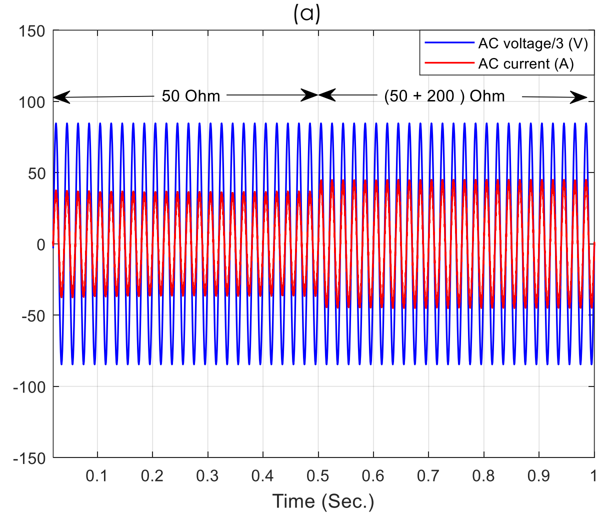

(b)

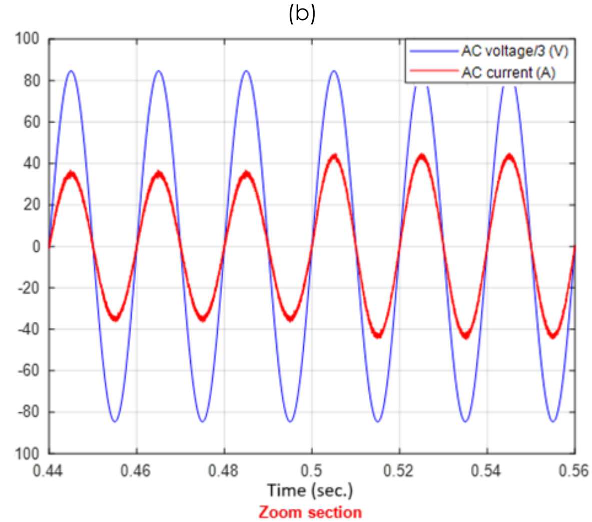

(c)

Figure 9 (a) DC output voltage and current waveform, (b) AC voltage and current waveform, and (c) it's zoom section

For a non-sinusoidal case (with non-sinusoidal voltages and/or currents), the following power components are defined: active power (P), fundamental active power component (P_1), DC power (P_{dc}), and total harmonic active power component (P_H).

$$P = P_1 + P_H + P_{\mathrm{dc}} \tag{6}$$

$$P_1 = V_1 I_1 \cos(\theta_1 - \phi_1) \tag{7}$$

$$P_H = \sum_{h=2}^{\infty} V_h I_h \cos(\theta_h - \phi_h) \tag{8}$$

$$P_{\mathrm{dc}} = V_{\mathrm{dc}} I_{\mathrm{dc}} \tag{9}$$

Where Φ_1, Φ_h, θ_1, and θ_h represent the phase angles of the supply voltage and current, respectively, at the fundamental component (1) and harmonic orders (h). The supply current and voltage at the fundamental order (i_1, v_1) and harmonic orders (i_h, v_h) are calculated as follows:

$$\left.\begin{aligned} i_1 &= \sqrt{2} I_1 \sin(wt - \phi_1), \quad i_h = \sqrt{2} \sum_{h=2}^{\infty} I_h \sin(h.wt - \phi_h) \\ v_1 &= \sqrt{2} V_1 \sin(wt - \theta_1), v_h = \sqrt{2} \sum_{h=2}^{\infty} V_h \sin(h.wt - \theta_h) \end{aligned}\right\} \tag{10}$$

The reactive power (Q), the fundamental reactive power component (Q_1), and the total harmonic reactive power component (Q_H) for a non-sinusoidal case are defined as:

$$\left.\begin{aligned} Q_1 &= V_1 I_1 \sin(\theta_1 - \phi_1) \\ Q_H &= \sum_{h=2}^{\infty} V_h I_h \sin(\theta_H - \phi_H) \end{aligned}\right\} \tag{11}$$

$$Q = Q_1 + Q_H \tag{12}$$

The apparent power (S), fundamental apparent power (S1), and total harmonic apparent power component (SH) for a non-sinusoidal case are defined as:

$$S_1 = V_1 I_1, \qquad and \qquad S_H = V_H I_H \tag{13}$$

$$S = S_1 + S_H \tag{14}$$

Distortion power is introduced only when the harmonic components of the corresponding voltage and current of different orders are multiplied. The total distortion power is calculated as follows:

$$D = \sqrt{\sum_{m \neq n = 1}^{\infty} V_m^{\ 2} I_n^{\ 2}} = \sqrt{S^2 - P^2 - Q^2} \tag{15}$$

According to these equations, the S, P, Q, and D powers are calculated at various DC output voltages, as illustrated in Figure 10. It can be seen from these waveforms that the reactive and distortion powers are almost zero, which confirms the unity power factor. Also, the apparent and active powers are aligned, which confirms this issue.

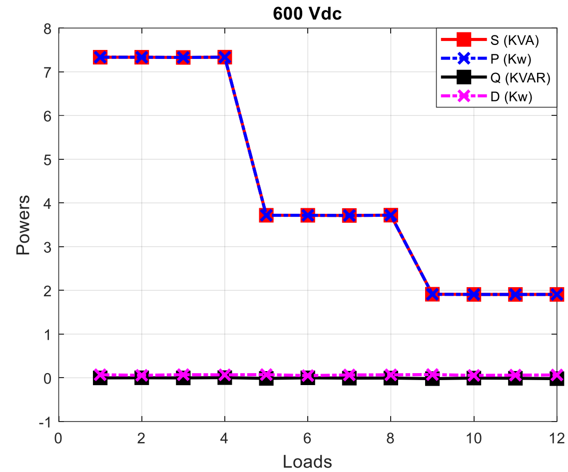

(a)

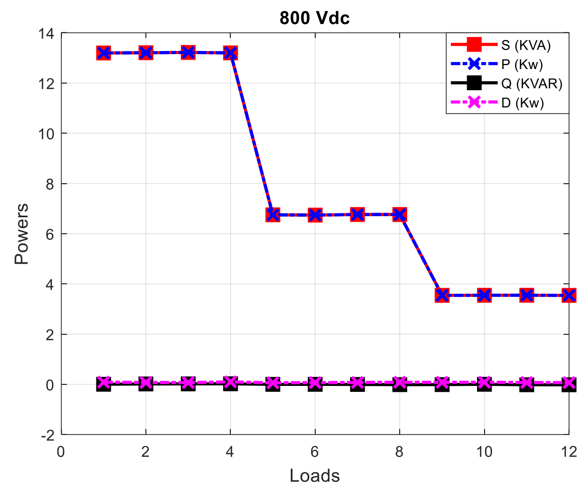

(b)

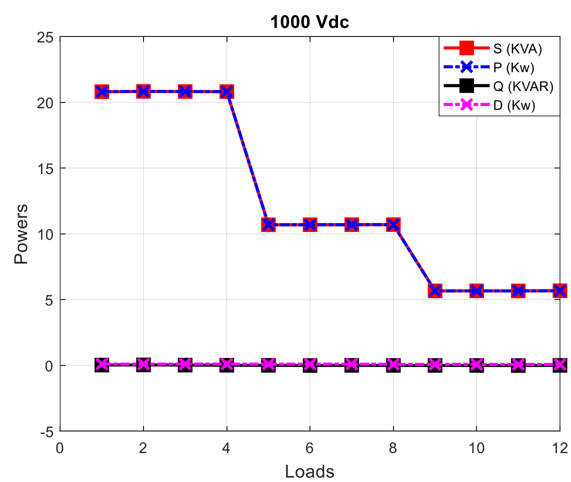

(c)

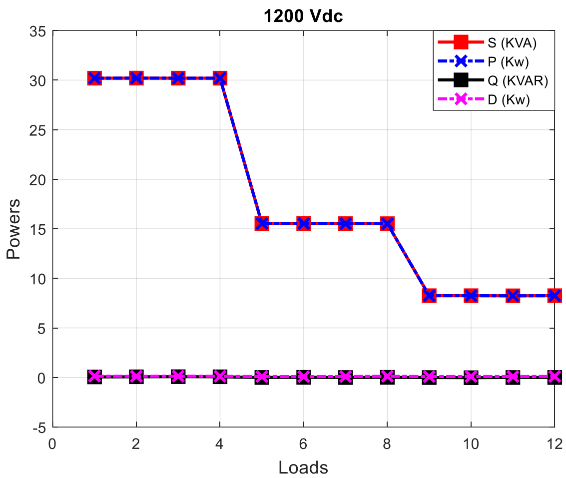

(d)

Figure 10 Apparent, active, reactive, and distortion powers results at (a) 600Vdc, (b) 800Vdc, (c) 1000Vdc, and (d) 1200Vdc at different loads

3.2 Distorted AC voltage Sources

The system is tested at 800Vdc and R=50Ω. In this case, the peak AC supply voltages are set at V_a = 241V, V_b = 271V, and V_c = 221V, as shown in Figure 11. The supply AC currents have THD values of 2.976%, 2.975%, and 2.9891%, as demonstrated in Figure 12. The DC voltage response in the unbalanced case is shown in Figure 13. The system still has an acceptable DC output response. To demonstrate the effectiveness of the suggested system, another unbalanced case is tested with V_a=381V, V_b=351V, and V_c=401V. The three-phase AC voltages and currents, along with the FFT analysis and the output DC voltage responses, are shown in Figures 14, 15, and 16. These waveforms show that the THD values of the three-phase supply currents are 2.5621%, 2.5472%, and 2.5409%. To assess the robustness of the proposed circuit, a worst-case scenario is tested. This scenario involves unbalanced voltages with peak values of 381V and distortion caused by the 5th harmonic order, as depicted in the Figures 17, 18, and 19. The THD value of the supply voltage is 27.566%, while the supply currents are 0.41569%, 0.37435%, and 0.3867%. The DC output voltage response still has a good response. The power factor is 0.9994 lagging, and the S, P, Q, and D are 13.84 kVA, 13.337 kW, -446 VAR, and 366W, respectively.

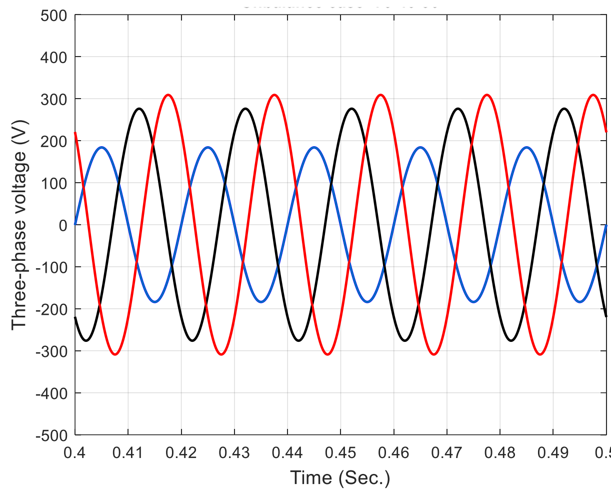

(a)

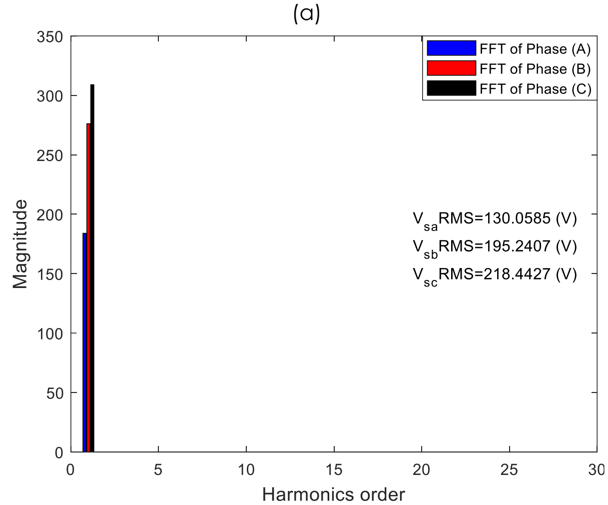

(b)

Figure 11 The unbalanced AC supply voltages with their FFT analysis

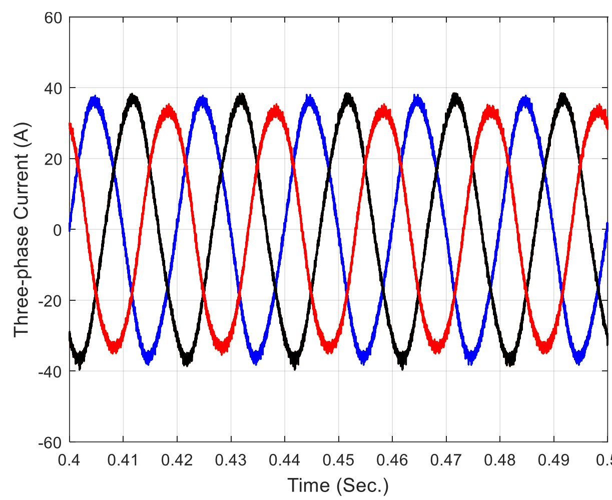

(a)

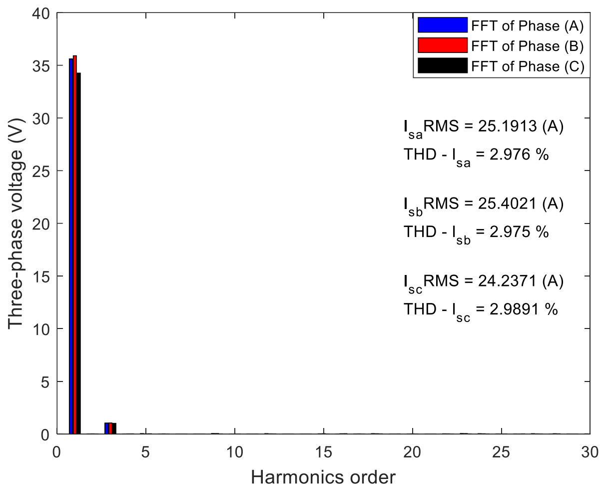

(b)

Figure 12 The three-phase AC currents and its FFT analysis during unbalanced AC voltages

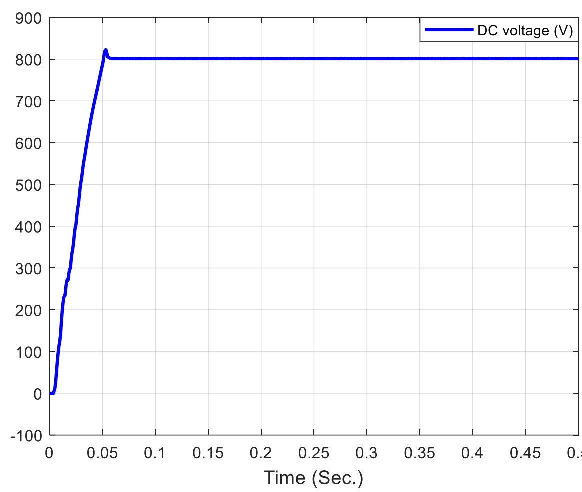

Figure 13 The DC voltage response during unbalanced case

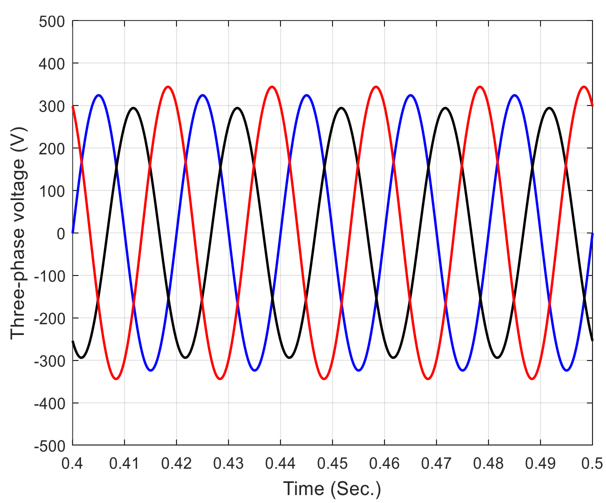

(a)

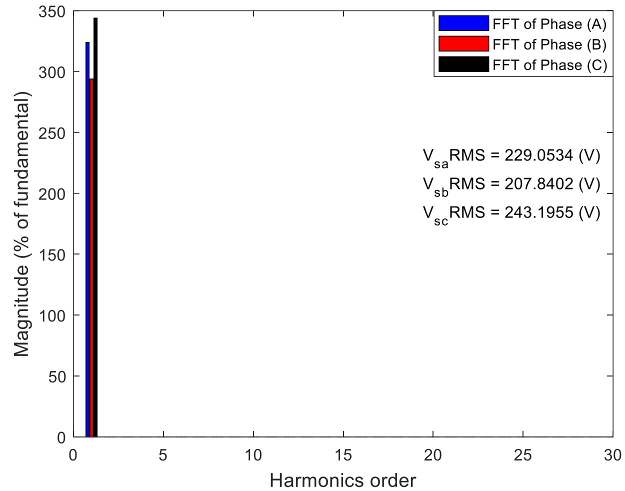

(b)

Figure 14 The unbalanced AC supply voltages with their FFT analysis

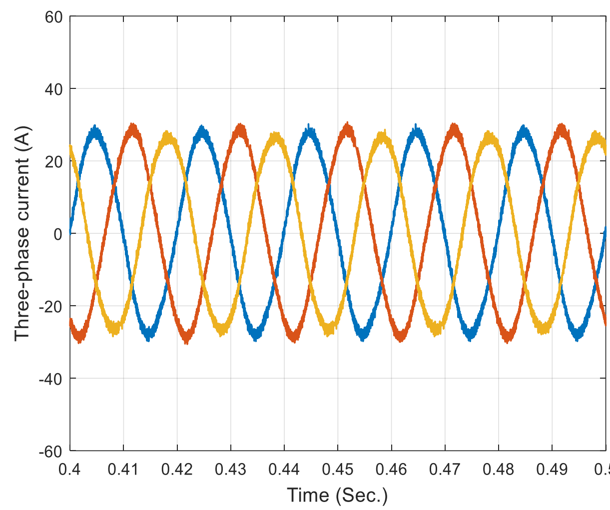

(a)

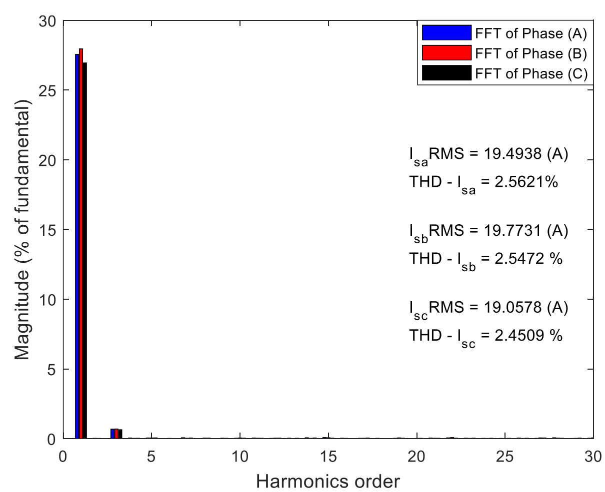

(b)

Figure 15 The three-phase AC currents and its FFT analysis during unbalanced AC voltages

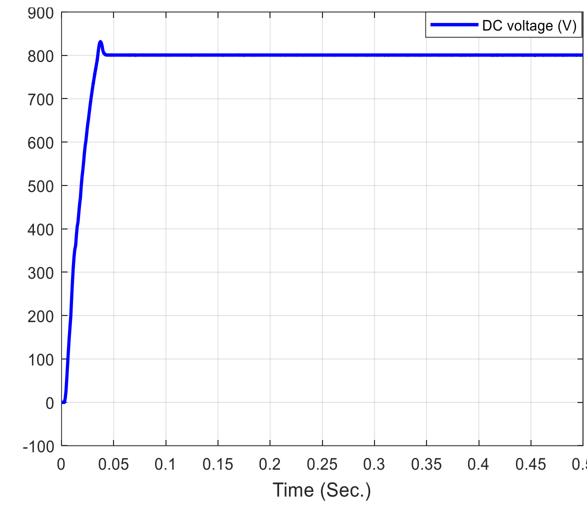

Figure 16 The DC voltage response during unbalanced case

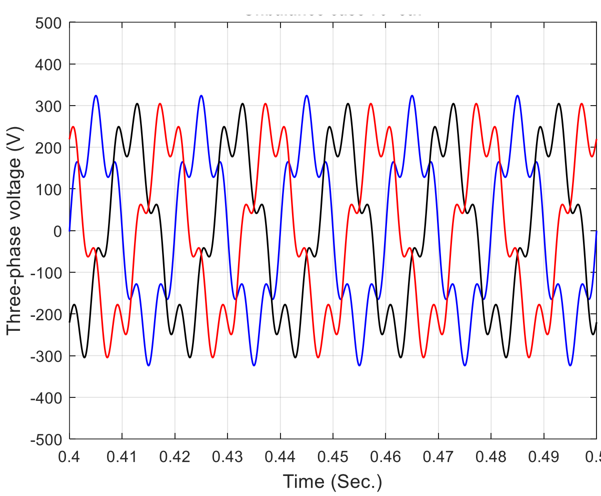

(a)

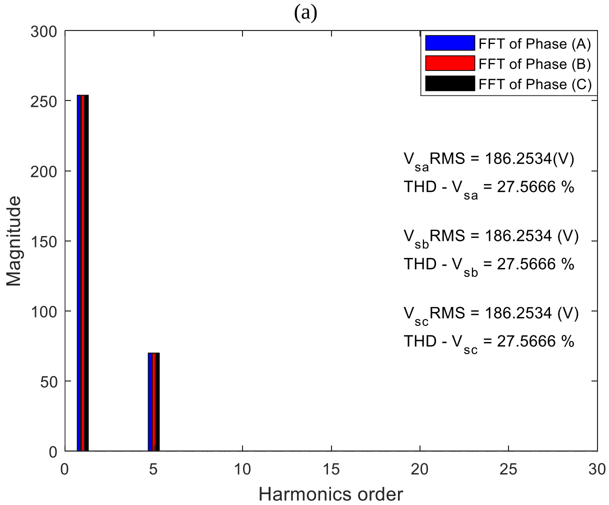

(b)

Figure 17 The unbalanced distorted AC supply voltages with its FFT analysis

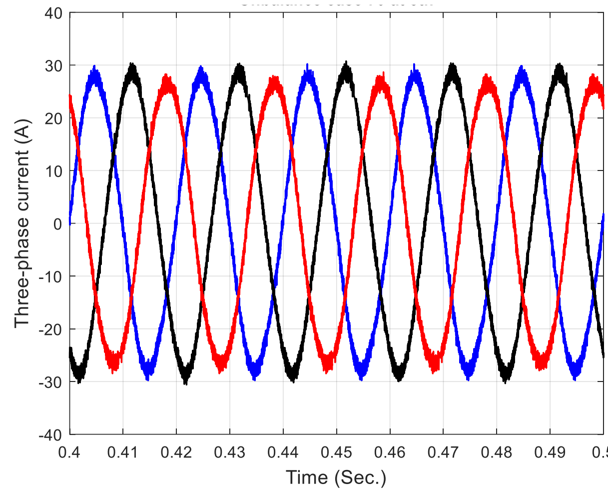

(a)

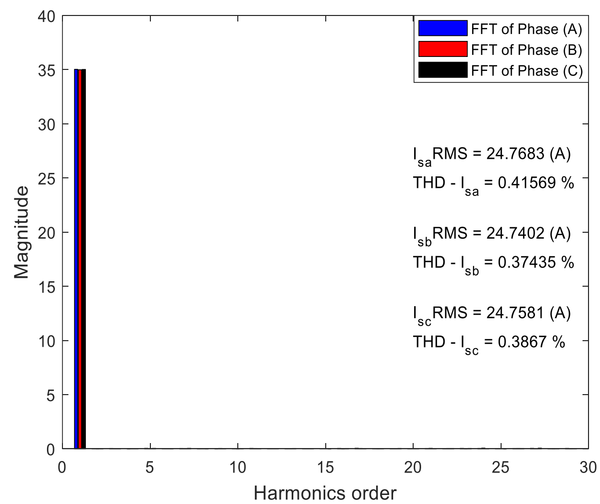

(b)

Figure 18 The three-phase AC currents and its FFT analysis during unbalanced and distorted AC voltages

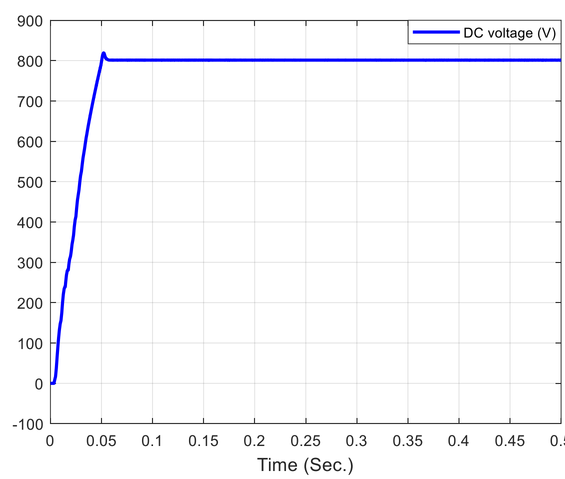

Figure 19 The DC voltage response during unbalanced and distorted case

4.0 CONCLUSIONS

In this study, a high power quality SPWMR circuit and controller have been suggested and modelled under various operating conditions. The system is tested with 12 different loads under balanced and unbalanced distorted AC sources in order to achieve low distortions, unity power factor, and a valuable output voltage with high responsiveness. At balanced AC supply voltages, the minimum and maximum current distrotion values are 0.3867% and 3.8992% at different output DC voltages and loads. During unbalance voltages, the minimum and maximum current distrotion values are 2.5409% and 2.976%. Whereas with unbalanced distorted AC supply voltages of THD 27.566%, the THD values of the three-phase supply currents are 0.41569%, 0.37435%, and 0.3867% with power factor of 0.999. From the modelling results, it can be noticed that the SPWMR with balanced and unbalanced AC supply, and distorted voltages with the 5th harmonic order gave acceptable results. All case studies demonstrate the system's performance by reducing the THD values and improving the power factor under various operating conditions. The quality of the designed system focuses on achieving balanced three-phase input AC currents, minimizing THDs to values less than 5%, achieving almost unity power factor, and regulating the output DC voltage at any desired value. Finally, the system response in both the transient and steady-state responses is good when using the designed and modelled system.

Acknowledgement

I want to thank the Northern Technical University and inform that these is no funding was received from outside sources.

Conflicts of interest

The author(s) declare(s) that there is no conflict of interest regarding the publication of this paper.

References

[1] Acikgoz, H., Kecécioglu O. F., Gani, A., Yildiz, C., Sekkeli, M. 2016. Improved Control Configuration of PWM Rectifiers based on Neuro-fuzzy Controller. *SpringerPlus.* 5: 1142. https://doi.org/10.1186/s40064-016-2781-5.

[2] Al-Badrani, H. Feuersaenger, S. and Pacas, M. 2018, VSI with Sinusoidal Voltages for an Enhanced Sensorless Control of the Induction Machine. *PCIM Europe 2018; International Exhibition and Conference for Power Electronics, Intelligent Motion, Renewable Energy and Energy Management, Nuremberg, Germany.* 1–7. https://doi.org/10.1109/SPEC.2018.8635854.

[3] Shneen, S. W., Aziz, G. A., Abdullah, F. N., Shaker, D. H. 2022. Simulation Model of 1-phase Pulse-width Modulation Rectifier by using MATLAB/Simulink. *International Journal of Advances in Applied Sciences* (IJAAS). 11(3): 253–262. https://doi.org/10.11591/ijaas.v11.i3.pp253-262.

[4] Mitra, A., Chowdhuri, S. 2017, Analysis of Single Phase PWM Rectifier for Different Applications. *Journal of The Institution of Engineers (India): Series B.* 98: 161–169, https://doi.org/10.1007/s40031-016-0217-9.

[5] Hartani, K., Miloud, Y. 2010, Control Strategy for Three Phase Voltage Source PWM Rectifier based on the Space Vector Modulation. *Advances in Electrical and Computer Engineering.* 10(3): 61–65. https://doi.org/10.4316/aece.2010.03010.

[6] Garasiya, D. V., Vora, S. C., Kapil, P. N. 2012. Simulation, design and practical realization of single phase PWM boost rectifier. *Nirma University International Conference on Engineering (NUiCONE), Ahmedabad, India*. 1–6. https://doi.org/10.1109/NUICONE.2012.6493272.

[7] Koshti, R., Purohit, D., Mehta, N. D. 2014. Design and Simulation of Three-phase Voltage Source Space Vector Based PWM Rectifier. *IJLTEMAS*. 3(5): 77–81.

[8] Hassan, T. K., Abdullah, M. K. 2015. Control Strategy for Three-phase PWM Boost Rectifier Operating Under Different Supply Voltage Conditions. *Iraq Journal of Electrical and Electronic Engineering.* 11(1): 83–100. https://doi.org/10.37917/ijeee.11.1.9.

[9] Qiang, W., Yong-bao, L., Xing, H., Qian-chao, L. 2017. Simulation Study of Three - phase PWM Rectifier with Square of the Voltage Double Closed Loop Control. *2nd Asia Conference on Power and Electrical Engineering (ACPEE 2017), IOP Conference Series: Materials Science and Engineering.* 199. https://doi.org/10.1088/1757-899X/199/1/012148.

[10] Soe, H. H., Naing, T. L. 2019. Simulation of Single-phase IGBTs H-bridge PWM Rectifier for R and RL Load with Hysteresis Current Control. *The Twelfth National Conference on Science and Engineering NCSE*, 2019. 342–346.

[11] Hashemzade, S. M., Rostami, R. Marzang, V., Hosseini, S. H. 2020. Direct Power Control of PWM Three-Phase Rectifier Using the Predictive Method: Aims to Reduce THD. *28th Iranian Conference on Electrical Engineering (ICEE), IEEE*. https://doi.org/10.1109/ICEE50131.2020.9261070.

[12] Song, T., Wang, P., Zhang, Y., Gao, F., Tang, Y., Pholboon, F. 2020. Suppression Method of Current Harmonic for Three-Phase PWM Rectifier in EV Charging System. *IEEE Transactions on Vehicular Technology.* 69(9): 9634–9642, https://doi.org/10.1109/TVT.2020.3005173.

[13] Yuksek, H. I., Arifoglu, U. 2020. Modeling of Three-phase Three-level Rectifier with Space Vector Pulse Width Modulation Method in Matlab/Simulink Program. *Sigma Journal of Engineering and Natural Sciences.* 38(1): 227–251. https://hdl.handle.net/20.500.12619/95347.

[14] Bie, Y., Li, Y., He, G., Zhang, X. 2021. PWM Rectifier Impedance Modelling and Analysis. *IOP Conf. Series: Earth and Environmental Science*. 675: 012064, https://doi.org/10.1088/1755-1315/675/1/012064.

[15] ISEN, E. 2021, Comparative Study of Single-Phase PWM Rectifier Control Techniques. *Mugla Journal of Science and Technology.* 7(1): 44–52. https://doi.org/10.22531/muglajsci.870989.

[16] Li, H., Cheng, G., Zhang, Y. 2021. Research on Three-phase PWM Rectifier based on Double Closed-loop Feed forward decoupling control. *Journal of Physics: Conference Series, IOP*. 1738(1). https://doi.org/10.1088/1742-6596/1738/1/012108.

[17] Wang, Z., Qu, Q., Zhang, Y., Min, Z. 2022. Model-Free Predictive Power Control for PWM Rectifiers under Asymmetrical Grids. *Symmetry,* 14(6): 1224. https://doi.org/10.3390/sym14061224.

[18] Zhou, Z., Song, J., Yu, Y., Xu, Q., Zhou, X. 2023. Research on High-quality Control Technology for Three-phase PWM Rectifier. *Electronics.* 12: 2417. https://doi.org/10.3390/electronics12112417.

[19] Irwanto, M., Nugraha, Y. T., Hussin, N., Nisja, I. 2023. Effect Of Temperature and Solar Irradiance on the Performance of 50 Hz Photovoltaic Wireless Power Transfer System. *Journal Teknologi.* 85(2): 53–67. https://doi.org/10.11113/jurnalteknologi.v85.18872.

[20] Tobing, S. W. L., Afdila, R., Panjaitan, P. E., Situmeang, N. C., Hutagalung K. N., Sidabutar, R. 2022. ABC to DQ Transformation for Three-Phase Inverter Design as Prime Mover Speed Control in Microgrid System. 2022 6th International Conference on Electrical, Telecommunication and Computer Engineering (ELTICOM), Medan, Indonesia. 70–74. https://doi.org/10.1109/ELTICOM57747.2022.10038242.

[21] Bi, K., Xu, Y., Zeng, P., Chen, W., Li, X. 2022, Virtual Flux Voltage-oriented Vector Control Method of Wide Frequency Active Rectifiers Based on Dual Low-Pass Filter. *World Electrical Vehicle Journal*. 13(2): 35. https://doi.org/10.3390/wevj13020035.

[22] ANTAR, R. K., Saied, B.M, Putrus, G. A., Khalil, R. A. 2021. Treating the Impacts of Connecting HVDC Link Converters with AC Power System Using Real-Time Active Power Quality Unit. e-Prime Journal. 1(2021): 100013. https://doi.org/10.1016/j.prime.2021.100013.

[23] Saied, B. M., Antar, R. K. 2010. The Investigation of Power Distortion in a Three-phase Modified Controlled Converter Circuit. *2010 7th International Multi-Conference on Systems, Signals and Devices, Amman, Jordan*. 1–6. https://doi: 10.1109/SSD.2010.5585595.